

ONLINE MEASUREMENT OF FLOUR PARTICLE SIZE DISTRIBUTION USING PIEZOELECTRIC SENSOR

*Nihat ÇANKAYA 

Necmettin Erbakan University, Meram Vocational School, Food Processing Department, Konya, TÜRKİYE
ncankaya@erbakan.edu.tr

Highlights

- Piezoelectric sensor was successfully used to measure the particle size of flour.
- 100% success was achieved in classifying five different types of flour mixtures.
- It was seen that the developed method could be used to improve the flour production process.

Graphical Abstract



Flowchart of the proposed method



ONLINE MEASUREMENT OF FLOUR PARTICLE SIZE DISTRIBUTION USING PIEZOELECTRIC SENSOR

*Nihat ÇANKAYA 

Necmettin Erbakan University, Meram Vocational School, Food Processing Department, Konya, TÜRKİYE
ncankaya@erbakan.edu.tr

(Received: 31.03.2024; Accepted in Revised Form: 14.10.2024)

ABSTRACT: Obtaining the ideal particle size is a vital factor in dust processes, from turning wheat into flour to cement and calcite production. However, the technology to measure particle size instantaneously during the production phase is still an area under development. These measurements made with electro-optical methods have limited use in industry due to their difficulties and excessive costs. Studies conducted with innovative acoustic emission sensors offer new hopes in particle size detection. These sensors can successfully measure the dimensions of a wide range of materials, from coal dust to metal powders to grass particles. Our study shows that these sensors can also measure the size of light flour particles instantaneously. Using developed method, the dimensions of five types of flour mixtures in the size ranges of 0-80 μm , 80-118 μm , 118-150 μm , 150-180 μm and 180-212 μm could be measured and classified with 100% success. Considering its potential to increase the efficiency of the milling process, this technology could revolutionize the milling industry.

Keywords: *Piezoelectric, Sensor, Acoustic Emission, Data Acquisition, Particle Size Distribution, Flour Milling*

1. INTRODUCTION

Today, many studies are conducted to increase energy efficiency in areas such as industry, housing, agriculture and transportation. In one application, the energy consumption of dust filters used in industry was reduced by 55% using the newly developed method [1]. Time and energy loss have been reduced by using new control software developed for the industrial sandblasting process [2]. Artificial intelligence algorithms have been developed to be used to increase energy efficiency in buildings [3]. Artificial intelligence-supported weather forecasting algorithms have been developed that can increase efficiency in agriculture and transportation [4], [5]. A vision for increasing energy efficiency was presented by examining the renewable energy resources in the world [6]. Optimization software and models have been developed for industrial production efficiency [7], [8], [9].

Research is being conducted in many different fields related to the structure of the piezoelectric materials used in this study and their use to increase efficiency in the industrial field. Existing piezoelectric materials have been examined and piezo-electric-chemical materials that can be used in chemical processes have been developed [10]. Factors affecting the performance of piezoelectric materials have been examined [11]. The chemistry of stretchable piezoelectric elastic composite materials that can be used in wearable technologies has been investigated [12]. Piezoelectric energy harvesters have been studied [13], [14]. The effects of acoustic sound waves produced by human footsteps on a piezoelectric element were examined [15]. Acoustic signals in cracks in layered titanium fabrication have been investigated using piezoelectric acoustic emission sensors [16]. A mathematical model using a piezoelectric sensor has been developed to examine the health of metallic and composite structures [17]. The propagation pattern of acoustic waves has been studied in metal and aluminum material environments [18]. An inexpensive piezoelectric sensor design that can be attached to the device surface has been proposed [19]. Polyvinylidene difluoride (PVDF) was doped with nanocomposite lead zirconate titanate (PZT) particles and a flexible piezoelectric pressure sensor was developed for energy harvesting applications [20]. A piezoelectric transducer was designed using cylindrical PZT [21]. Piezoelectric acoustic devices based on commonly used piezoelectric materials have been reviewed [22]. A method that uses piezoelectric PZT

*Corresponding Author: Nihat ÇANKAYA, ncankaya@erbakan.edu.tr

material and can measure the energy of laser light by converting light waves into sound waves has been developed [23]. A piezoelectric bed impact load sensor was developed to estimate the mass and particle size distribution of bed load in naturally sloping streams [24]. The sizes of sand and stones in the rivers were measured with a piezoelectric sensor specially placed in the riverbed, and environmental changes were analyzed to take precautions for future disasters [25]. A piezoelectric-based coating material that can positionally detect real-time impact on planes structural parts has been developed [26].

It is especially important measuring particle sizes and keeping them within certain limits for efficiency in industrial production processes. For example, the certain size of bioparticles and powdered coal is highly effective on combustion efficiency, in biofuel and coal power plants. In metal, ceramic or plastic production facilities, it is necessary to measure particle sizes to ensure good mixing. Excessive grinding of flour in flour production facilities damages the flour and causes the machine to consume too much energy. The size of the particles must be measured instantly in many production processes such as cement and detergent production. Although electro-optical methods are available, their excessive cost is a disadvantage. At this point, piezoelectric materials can be used to measure particle size in industrial production processes. A specially designed piezoelectric-based sensor is installed in the flow pipe through which the coal dust passes. Impact experiments were conducted with glass particles and coal particles of sizes 64 μ , 74 μ , 103 μ and 133 μ at different speeds by the sensor. As a result, it was seen that as the size of the particles increases, the amplitude durations resulting from the impact increase. Likewise, it has been seen that amplitude durations increase as impact speeds increase [27]. It has been shown that the dimensions of steel, cast iron and aluminum powders ranging in size from 0.15 to 1.1 mm can be measured with piezoelectric-based sensors. The signal generated by particles falling freely from different heights into the aluminum waveguide to which the sensor is connected was passed through an amplifier and then examined by counting the amplitudes in 4 channels with different frequencies and threshold ranges [28]. With the established experimental setup, particle mixtures of 4-16 mm in size were dropped from different heights in free fall and hit the metal waveguide to which a piezoelectric-based acoustic emission sensor was connected. The signals resulting from the impact were sampled with a high-speed digitizer and the frequency spectrum of the resulting signal was examined. According to the results obtained, it has been seen that mixtures with a high proportion of small particles have larger amplitudes at higher frequencies, and mixtures with a high proportion of large particles have amplitude maximums at low frequencies [29]. The ratio of particles belonging to willow and miscanthus plants, which are used in energy production with biomass and whose sizes vary between 400 and 5000 μ , in the mixture was measured instantly with a piezoelectric sensor. The effect of different speeds and mass flow rates on measurement was examined [30]. The proportions of glass powders between 20 and 250 μ in the mixture were measured with a piezoelectric-based acoustic emission sensor. The acoustic emission sensor connected to a metal waveguide placed in a flow pipe is sized according to the amplitude levels in the signal resulting from the impact of the particles. They see that their amplitude increases as the particle size increases [31]. The impact effects of small dust particles on lead zirconate titanate (PZT) ceramics have been studied [32]. The effect of granular materials of varied sizes on the piezoelectric PVDF film was examined through signal analysis [33]. In an experiment where a total of five sets of glass beads with average diameters of 0.4, 0.6, 0.8, 1.0 and 1.2 mm were used and the impact velocities varied between 22 m/s and 37 m/s, it was found that the Stronge impact theory described the impact process more accurately than the Hertz impact theory [34]. A new measurement system was developed using silica sands of sizes 116–750 μ m, 61–395 μ m and 10–246 μ m as test particles, respectively. Experiments have shown that Sperman's correlation coefficient is greater than 0.8 in all size ranges [35]. A particle sizing algorithm was developed in which parameters such as peak amplitude, number, width, rise time, and energy of the acoustic emission signal were included. In experiments with glass beads in the range of 0.4 mm to 1.2 mm, it was shown that particle sizes could be measured with a relative error of 10% [36]. In experiments where glass and polyethylene particles with sizes ranging from 150-212 μ m and 150-250 μ m were used as measurement materials and the free fall method was used on a plate to which an acoustic emission sensor was attached, it was shown that the particle size distribution in the mixture could be calculated with a time-domain based multiple

threshold algorithm [37], [38].

In this study, the use of piezo acoustic sensors in measuring the particle size distribution of light materials such as wheat flour was investigated, taking as reference the measurement of particle size distribution of heavy materials such as salt, sand, glass dust, coal dust and aluminum dust by piezo acoustic methods.

2. MATERIAL AND METHODS

2.1. Piezoelectric Element and Piezoelectric Effect

A piezo element with a diameter of 9 mm was glued to a steel waveguide and placed in the flow pipe of a vacuum cleaner with the help of a plastic apparatus produced by a 3D printer. Particle impact experiments were conducted at air flow velocities of 10 m/s and 20 m/s, and the signals produced in the piezo element were analyzed with the help of the developed peak amplitude detection and counting algorithm. In the experiments, a 9 mm diameter piezoelectric element, shown in Figure 1 was used to produce signals by the piezoelectric effect caused by the impact of flour particles. The experiments were repeated with piezoelectric elements of 12 mm and 20 mm diameter, but no significant difference was seen. The 9 mm diameter piezo element was selected due to its suitability for installation. The black wire was soldered to a brass plate of 9 mm diameter. This was the negative electrode and was numbered 1 in Figure 1. On the brass layer, there was a 7 mm diameter PZT piezoceramic layer numbered 2, which produces an electrical signal when pressure was applied. On this layer, there was a 6 mm diameter silver layer numbered 3, to which the positive electrode was soldered.

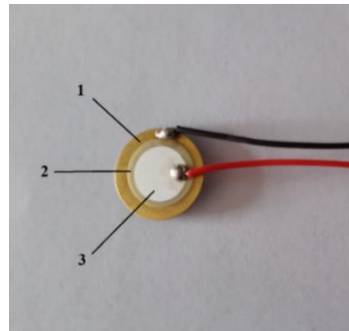


Figure 1. 9 mm piezoelectric element (1) 9 mm diameter, brass layer (2) 7 mm diameter, PZT piezo ceramic layer (3) 6 mm diameter, silver layer

The direct piezoelectric effect, in which mechanical energy is converted into electrical energy, is explained by the equations given below. The relationship between polarization and stress is expressed as in Equation (1). The electrostatic equation of a capacitor is given in Equation (2). Since polarization means field per charge, it is expressed by Equation (3).

$$P = d\sigma \quad \text{where:} \quad (1)$$

P = polarization
 d = piezoelectric coefficient
 σ = stress

$$Q = CV \quad \text{where:} \quad (2)$$

Q = charge
 C = capacitance
 V = voltage

$$P = \frac{Q}{A} \quad \text{where:} \quad (3)$$

P= polarization
 Q= charge
 A= area

Since stress (σ) is force per area, Equation (4) is obtained.

$$\sigma = \frac{F}{A} \quad \text{where:} \quad (4)$$

σ = stress
 F= force
 A= area

If we substitute Equation (3) and Equation (4) into Equation (1), we obtain Equation (5). These equations tell us that if we apply the same force to the piezoelectric material over a small or large area, we will obtain the same voltage.

$$Q = dF \quad \text{where:} \quad (5)$$

Q= charge
 d= piezoelectric coefficient
 F= force

Since voltage is generally used in sensor applications, we substitute Equation (2) into Equation (5) and obtain Equation (6).

$$V = \frac{dF}{C} \quad \text{where:} \quad (6)$$

V= voltage
 d= piezoelectric coefficient
 F= force
 C= capacitance

The capacitance of the material is obtained with Equation (7).

$$C = \frac{\epsilon_0 \epsilon_r A}{t} \quad \text{where:} \quad (7)$$

C= capacitance
 ϵ_r = relative permittivity
 ϵ_0 = vacuum permittivity
 A= area
 t= thickness

If we substitute Equation (7) into Equation (6), we obtain the piezoelectric working equation in terms of voltage given in Equation (8).

$$V = \frac{dFt}{\epsilon_0 \epsilon_r A} \quad \text{where:} \quad (8)$$

V= voltage
 d= piezoelectric coefficient
 F= force

- t = thickness
- ϵ_r = relative permittivity
- ϵ_0 = vacuum permittivity
- A = area

2.2. Experimental Setup

A vacuum cleaner was used to provide the airflow necessary to accelerate the flour particles. The piezoelectric sensor was not directly exposed to the particles. It was attached to a metal waveguide with a strong adhesive, and the metal waveguide was placed in the air flow pipe as shown in Figure 2 and Figure 4. For this purpose, the plastic part shown in Figure 3 was designed and then manufactured with the Creality Ender 5 Plus 3D printer. Plastic designs with dimensions of 35x35x40 cm could be produced with the Creality Ender 5 plus 3D printer. ABS type plastic material was used as raw material due to its suitable properties such as high-temperature resistance, lightness and flexibility.

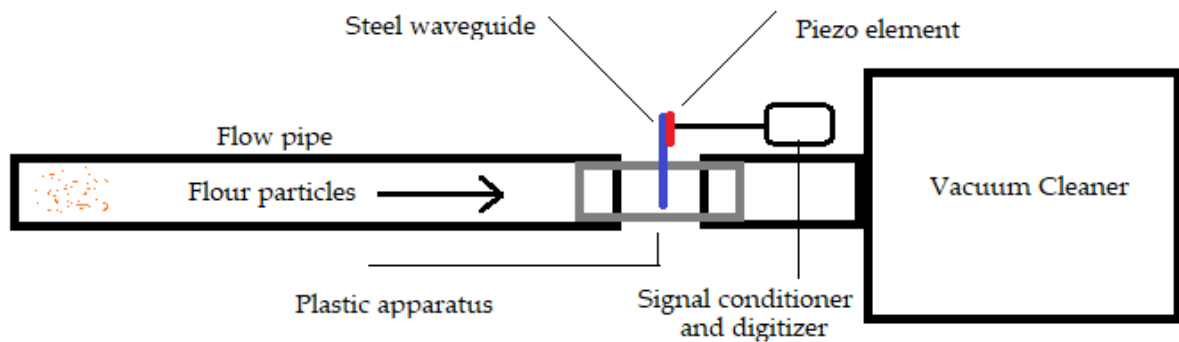


Figure 2. Schematic of experimental setup

Figure 3. (b) shows the position where the piezoelectric element was glued to the metal waveguide and the position where the waveguide was placed on the plastic apparatus. As seen in Figure 4. (a) and Figure 4. (b), all components were placed in the air flow pipe.

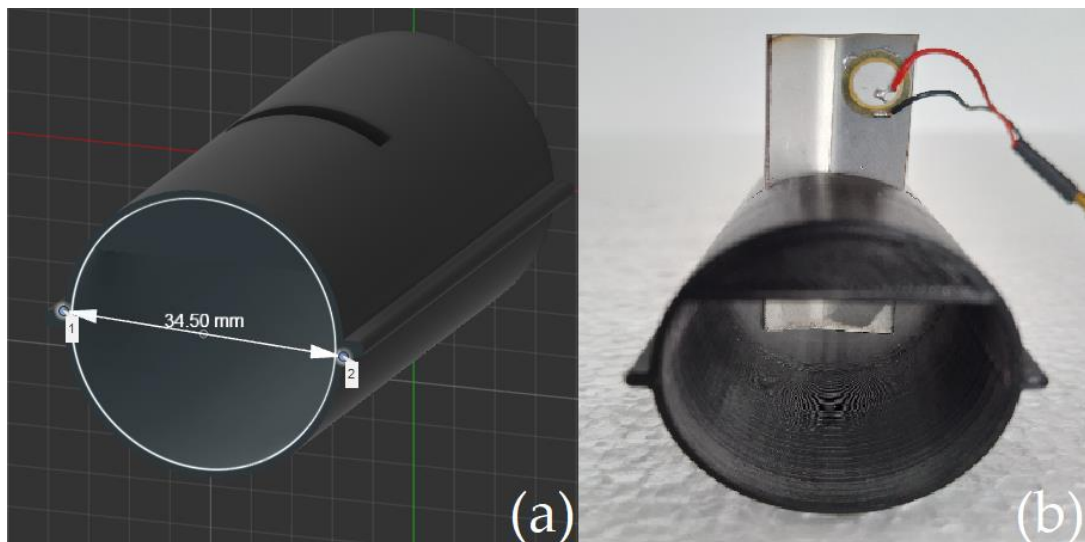


Figure 3. (a) Designed 3d printable plastic mounting apparatus (b) placement of piezoelectric element and metal waveguide on the mounting apparatus

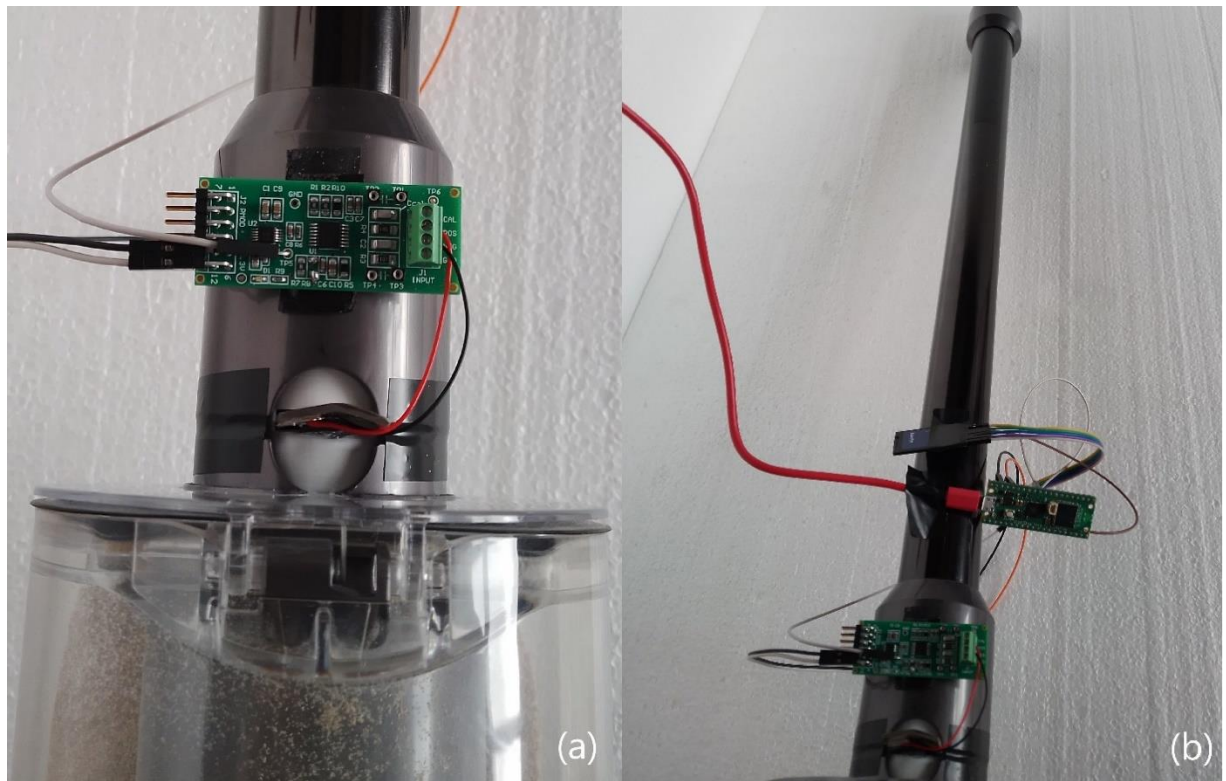


Figure 4. (a) Placement of the plastic mounting apparatus on the air flow pipe (b) air flow pipe

2.3. Data Acquisition Method

Since the signals generated in the piezoelectric element because of the particles hitting the metal waveguide were weak, signals were first passed through the amplifier circuit. In addition to hardware filtering, a software bandpass filter was used to cut noise in the signal. Using a microcontroller, the analog signal was converted to digital data and stored in an SD card. The data taken to the computer via the SD card was analyzed using the MATLAB program and a program written in Python language. A diagram of this process is given in Figure 5.



Figure 5. Data acquisition and analysis process chart

The amplitude of the electrical signals received from the piezoelectric element was increased by passing through an amplifier circuit. For this process, Analog Devices' amplifier circuit is shown in Figure 6 was used. Op-amp number U1A is a charge amplifier that converts the input current from the piezo element into voltage. The op-amp numbered U2A is a voltage amplifier with gain that can be adjusted with the R8 resistor. R6 and C8 elements in this circuit filter the output signal.

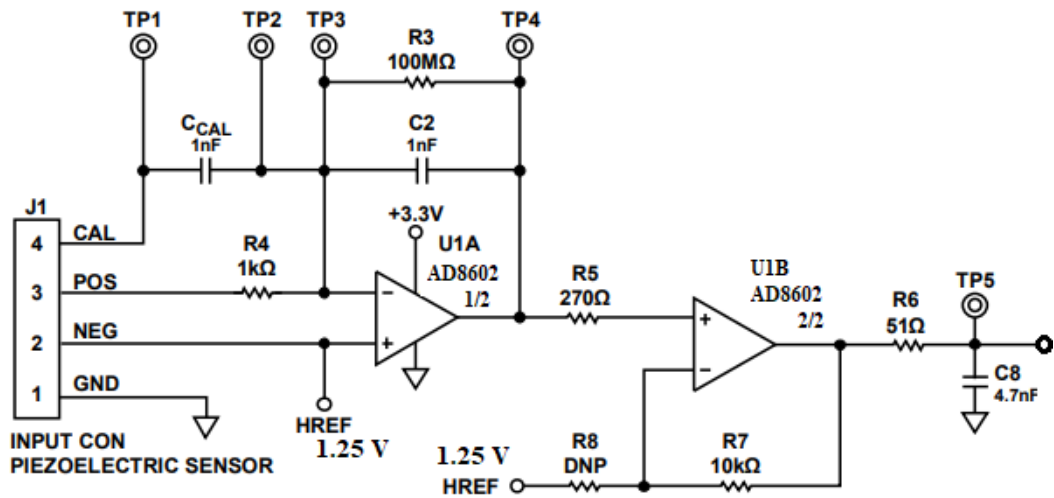


Figure 6. Signal Conditioning Circuit

A Raspberry Pi Pico WH card having an RP2040 microcontroller was used to convert the analog signal to digital data and save it to the SD card. One of the 3 ADC (Analog-Digital Converter) pins on the card with a sampling rate of 500 kps (kilo sample per second) at 12-bit resolution was used for this process. In each experiment, 15000 sample data were taken at 100 kps and recorded on a microSD card using the SPI communication method and the connection diagram given in Figure 7. The value of 15000 pieces of data recorded on the SD card varies between 0-4095 since it has 12-bit resolution. That is, amplitude values between 0-3.3 V are scaled in the range 0-4095. DMA (Direct Memory Access) method was preferred to take uninterrupted samples in the ADC process. The data recorded on the SD card was transferred to a computer for analysis. Signals were analyzed by developing software in MATLAB signal analyzer app and python programming language.

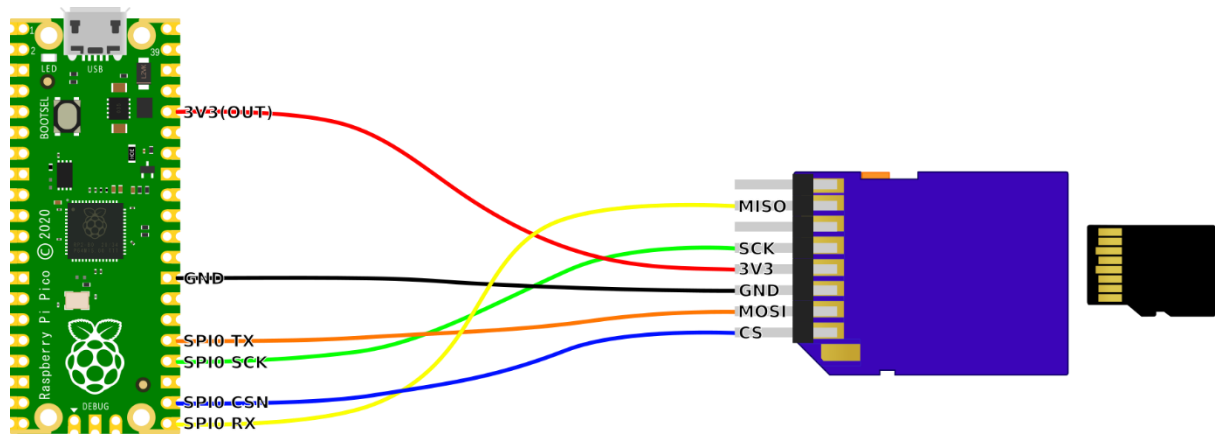


Figure 7. SPI communication connection between microSD card and microcontroller

2.4. Sizing of Flour Particles by Sieve Machine

A laboratory type sieve machine was used to sift the flour mixture to be used in the experiments and separate it into varied sizes. The whole wheat flour mixture was separated according to its size using the flour sifting machine shown in Figure 8. (a) and sieves of 80 μ , 118 μ , 150 μ , 180 μ and 212 μ sizes. The size ranges of the sifted flour particles are 0-80 μ m, 80-118 μ m, 118-150 μ m, 150-180 μ m and 180-212 μ m.

Additionally, flour mixtures with intermediate values were obtained by mixing flour mixtures of similar sizes half and half. For example, an intermediate flour mixture was obtained by taking equal proportions of flours in the size range of 150-180 μ and 180-212 μ and mixing them homogeneously. As seen in Figure 8. (b), flour mixtures placed in separate storage containers were used in the experiments.

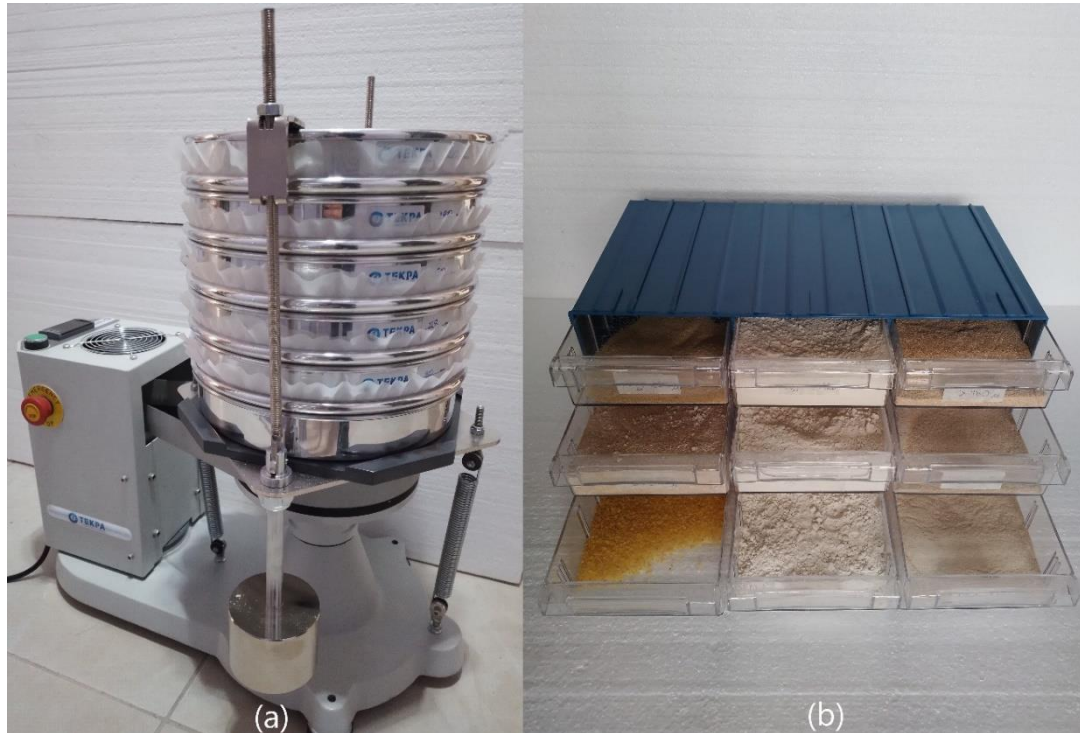


Figure 8. (a) Sifter machine and sieves (b) flour mixtures separated by sizes

3. RESULTS

Figure 9 shows the signal amplitudes generated in the piezoelectric element because of different sized flour particles hitting the waveguide at a speed of 10 m/s when the vacuum cleaner is used. The vertical axis shows the amplitude values scaled between 0-4095 due to ADC and the horizontal axis shows the number of samples.

The values in the signals in the range of 0-4095 were scaled to the voltage range of 0-3.3 V and divided into threshold ranges of 0.16 V. A peak amplitude finding and counting algorithm was developed to examine how many peaks occur in the specified voltage ranges. Figure 10 shows the number of peak amplitudes corresponding to the voltage ranges. There are two important findings from the experiment. First, it was seen that with the proposed measurement technique, light particles such as wheat flour can produce amplitudes in the piezo element like the relatively heavy particles in other studies. The second result is that as the size of the flour particles increases, the amplitudes of the signals they produce also increase. This is expected. As the size, mass or speed of the particles increases, the impact force they create when they hit the waveguide will also increase. This will cause the voltage amplitudes generated by the piezoelectric element to increase.

Experiments were also conducted at a speed of 20 m/s to investigate the effect of particle impact velocities on the produced signals. As seen in Figure 11, when particles in the same size range hit the waveguide at a speed of 20 m/s, the number of peak amplitudes in higher voltage ranges increases. For example, when the peak amplitude numbers created by flour particles in the size range of 180-212 μ m at a speed of 20 m/s are examined, the peak amplitude numbers in the range of 0.16-0.80 V decrease, while

those in the range of 0.80-1.70 V increase. Similarly, for particles of other sizes, the peak amplitude numbers decrease in low voltage ranges and increase in high voltage ranges.

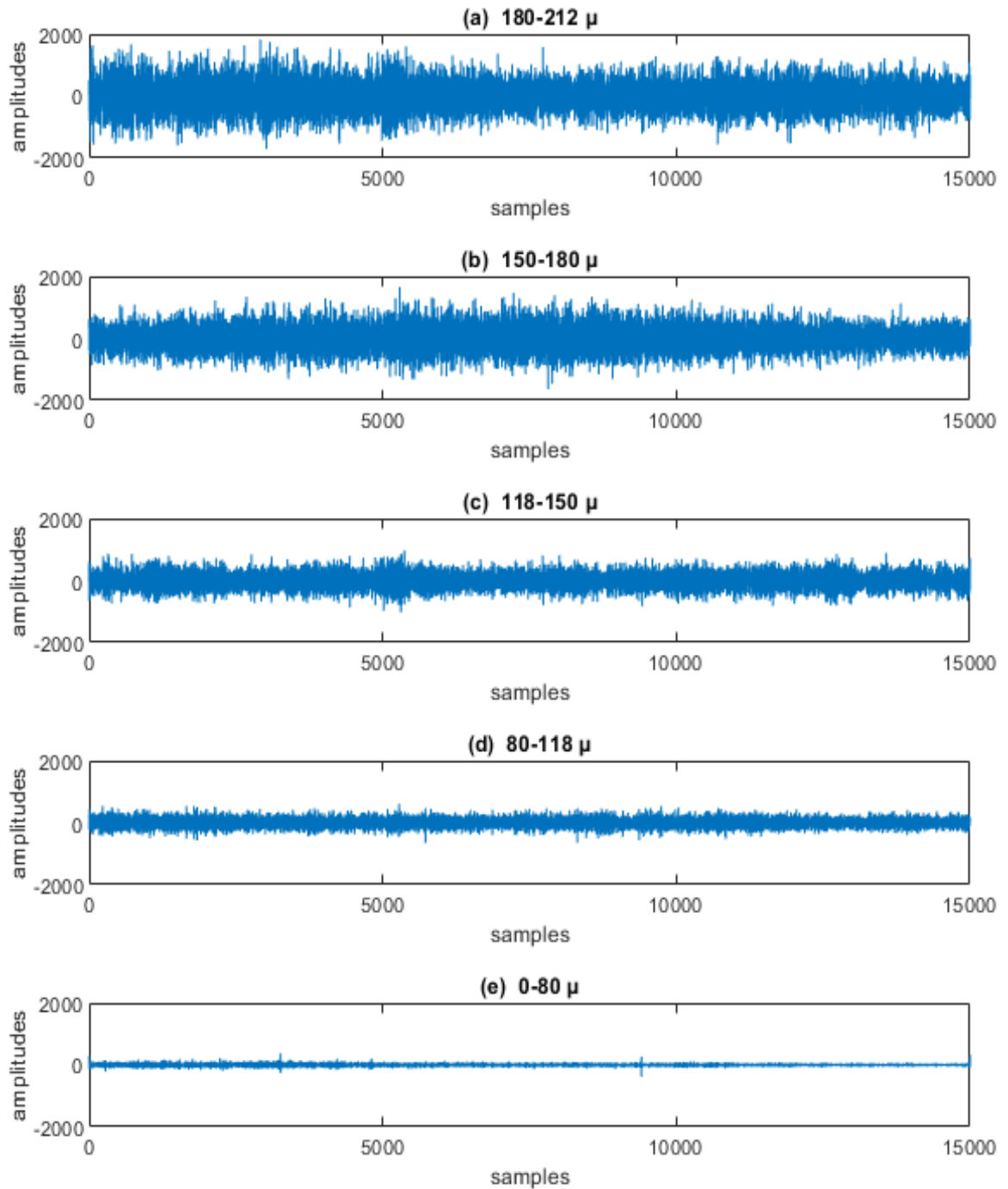


Figure 9. (a) Signal amplitudes for 180-212 μm (b) signal amplitudes for 150-180 μm (c) signal amplitudes for 118-150 μm (d) signal amplitudes for 80-118 μm (e) signal amplitudes for 0-80 μm

Voltage Ranges	Peak Counts by Voltage Ranges								
1.56-1.70	0	0	0	0	0	0	0	0	0
1.40-1.56	1	2	0	0	0	0	0	0	0
1.26-1.40	8	4	1	0	0	0	0	0	0
1.10-1.26	21	24	2	0	0	0	0	0	0
0.96-1.10	58	55	28	0	0	0	0	0	0
0.80-0.96	140	97	76	3	0	0	0	0	0
0.64-0.80	177	190	171	18	9	1	0	0	0
0.48-0.64	194	192	243	149	121	38	1	0	0
0.32-0.48	81	97	151	360	354	174	71	0	0
0.16-0.32	12	19	20	149	187	305	528	50	4
0.00-0.16	0	1	0	3	4	34	87	642	680
flow speed(m/s)	10	10	10	10	10	10	10	10	10
fleur sizes(μ)	180-212	180-212	150-180	150-180	118-150	118-150	80-118	80-118	0-80
		150-180		118-150		80-118		0-80	
mixture ratios	100	50:50	100	50:50	100	50:50	100	50:50	100

Figure 10. Peak counts by voltage ranges at 10 m/s

Voltage Ranges	Peak Counts by Voltage Ranges									
1.56-1.70	0	6	0	1	0	0	0	0	0	0
1.40-1.56	1	11	0	11	0	0	0	0	0	0
1.26-1.40	8	45	1	16	0	0	0	0	0	0
1.10-1.26	21	85	2	71	0	11	0	0	0	0
0.96-1.10	58	135	28	105	0	44	0	2	0	0
0.80-0.96	140	190	76	151	0	99	0	6	0	1
0.64-0.80	177	136	171	146	9	193	0	45	0	1
0.48-0.64	194	71	243	135	121	237	1	195	0	7
0.32-0.48	81	15	151	53	354	96	71	305	0	89
0.16-0.32	12	11	20	3	187	10	528	125	4	380
0.00-0.16	0	0	0	0	4	0	87	1	680	203
flow speed(m/s)	10	20	10	20	10	20	10	20	10	20
fleur sizes(μ)	180-212	180-212	150-180	150-180	118-150	118-150	80-118	80-118	0-80	0-80

Figure 11. Peak counts by voltage ranges at 20 m/s

4. DISCUSSIONS

The wheat flour particles used in the experiments were light particles, unlike the particles used in other studies such as salt, sand, glass dust, coal dust, aluminum dust. The most important feature of the study was that the sizes of light flour particles, especially in the range of 0-118 μm , could be measured with the proposed measurement technique. The counting results in Figure 11 were analyzed for a speed of 10 m/s, the voltage ranges with the highest counting values were accepted as thresholds and size classification was performed. Here, the voltage threshold values were decided as 0.00-0.16 V, 0.16-0.32 V, 0.32-0.48 V, 0.48-0.64 V and 0.64-0.80 V for particle size ranges of 0-80 μm , 80-118 μm , 118-150 μm , 150-180 μm and 180-212 μm , respectively. It was seen that the threshold values increase when the speed was 20 m/s. Since the type of flour in industrial production was decided by the particles being within a certain size range, here five distinct size ranges of flour types were classified as 100% successful. In addition, it was thought that flour production in the desired size range could be achieved by calibrating the voltage threshold values according to the flow speed. Differences in waveguides, piezo elements, amplifier gains, flow rates, particle sizes and types make direct comparison with other studies difficult. In addition, signals have been analyzed from different perspectives such as peak width and frequency in some studies. However, the common result of all studies is that as the particle size and flow rate increases, the amplitudes of the signals produced also increase [27], [28], [29], [30], [31], [34], [35], [36], [37].

5. CONCLUSIONS

In this article, a piezoelectric-based pulse detection system was presented to instantly measure the size of light flour particles of varied sizes. The increase in amplitude values was measured due to the increase in particle sizes and impact speed. Using developed method, five types of flour mixtures were classified with 100% success. It was possible that this system could be applied to industry.

In future studies, better results could be obtained by using metal waveguides and piezoelectric elements made of varied materials and with different geometric designs in the sensor structure. In signal analysis, it was predicted that more successful results could be obtained if amplitude duration analysis and frequency analysis were added in addition to amplitude level analysis.

DECLARATION OF ETHICAL STANDARDS

The author declares that he follows all scientific ethical rules, including authorship, citation and accuracy of data.

CREDIT AUTHORSHIP CONTRIBUTION STATEMENT

Author1: Finding the problem and deciding the solution proposal, researching and supplying the experimental materials, conducting experiments, developing software, preparing the draft of the article, writing and reviewing the article.

DECLARATION OF COMPETING INTEREST

The author declares that he has no conflict of interest.

FUNDING / ACKNOWLEDGEMENTS

This study was supported in part by TUBITAK under Grant Nr. 7230091.

DATA AVAILABILITY

All data was not presented in the article. It would be supplied by the author upon request.

6. REFERENCES

- [1] N. Çankaya and M. Özcan, "Performance optimization and improvement of dust laden air by dynamic control method for jet pulsed filters," *Advanced Powder Technology*, vol. 30, no. 7, pp. 1366–1377, Jul. 2019, doi: <https://doi.org/10.1016/j.apt.2019.04.014>.
- [2] A. Akkaş and M. Özcan, "Askılı Kumlama Makinesinin PLC İle Kontrolü Sayesinde Elde Edilen Kazanımlar," 2019. Accessed: Mar. 30, 2024. [Online]. Available: <https://dergipark.org.tr/tr/download/article-file/878177>
- [3] Mehmet HACİBEYOĞLU, Merve ÇELİK, and Özlem ERDAŞ ÇİÇEK, "K En Yakın Komşu Algoritması ile Binalarda Enerji Verimliliği Tahmini," *Necmettin Erbakan Üniversitesi Fen ve Mühendislik Bilimleri dergisi*, Dec. 2023, doi: <https://doi.org/10.47112/neufmbd.2023.10>.
- [4] Fatih ÖZEN, Rana ORTAÇ KABAOĞLU, and Tarık Veli MUMCU, "Deep Learning Based Temperature and Humidity Prediction," *Necmettin Erbakan Üniversitesi Fen ve Mühendislik Bilimleri dergisi*, Dec. 2023, doi: <https://doi.org/10.47112/neufmbd.2023.20>.
- [5] Muhammet Emre Irmak and İbrahim Berkan Aydilek, "Hava Kalite İndeksinin Tahmin Başarısının Artırılması için Topluluk Regresyon Algoritmalarının Kullanılması," *Academic platform-Journal of engineering and science*, pp. 507–514, Sep. 2019, doi: <https://doi.org/10.21541/apjes.478038>.
- [6] M. Bilgili, A. Ozbek, B. Sahin, and A. Kahraman, "An overview of renewable electric power capacity and progress in new technologies in the world," *Renewable and Sustainable Energy Reviews*, vol. 49, pp. 323–334, Sep. 2015, doi: <https://doi.org/10.1016/j.rser.2015.04.148>.
- [7] M. Karakoyun et al., "Fen ve Mühendislik Bilimleri Dergisi Transfer Fonksiyonları Kullanarak İkili Güve-Alev Optimizasyonu Algoritmalarının Geliştirilmesi ve Performanslarının Karşılaştırılması Development of Binary Moth-Flame Optimization Algorithms using Transfer Functions and Their Performance Comparison," 2021. Accessed: Mar. 20, 2024. [Online]. Available: <https://dergipark.org.tr/tr/download/article-file/1973003>
- [8] Barış GÖKÇE and Osman Bahadır ÖZDEN, "Kaynaklı Bağlantıya Sahip Karmaşık Bir Yapıda Goldak Modeli Kullanılarak Distorsiyonların ve Kalıntı Gerilmelerin Nümerik Analizler ile Belirlenmesi," *Necmettin Erbakan Üniversitesi Fen ve Mühendislik Bilimleri dergisi*, Dec. 2023, doi: <https://doi.org/10.47112/neufmbd.2023.9>.
- [9] M. S. Endiz and R. Akkaya, "Yarı Empedans Kaynaklı İnverterlerde Farklı PWM Kontrol Tekniklerinin Performans Etkisinin İncelenmesi," *Necmettin Erbakan Üniversitesi Fen ve Mühendislik Bilimleri Dergisi*, vol. 2, no. 1, pp. 12–26, Jun. 2020, Accessed: Mar. 20, 2024. [Online]. Available: <https://dergipark.org.tr/tr/pub/neufmbd/issue/55688/691719>
- [10] W. Qian, W. Yang, Y. Zhang, C. R. Bowen, and Y. Yang, "Piezoelectric Materials for Controlling Electro-Chemical Processes," *Nano-Micro Letters*, vol. 12, no. 1, Jul. 2020, doi: <https://doi.org/10.1007/s40820-020-00489-z>.
- [11] P. Eltouby, I. Shyha, C. Li, and J. Khaliq, "Factors affecting the piezoelectric performance of ceramic-polymer composites: A comprehensive review," *Ceramics International*, vol. 47, no. 13, pp. 17813–17825, Jul. 2021, doi: <https://doi.org/10.1016/j.ceramint.2021.03.126>.
- [12] J. Enrico et al., "Stretchable piezoelectric elastic composites for sensors and energy generators," *Composites Part B: Engineering*, vol. 198, pp. 108211–108211, Oct. 2020, doi: <https://doi.org/10.1016/j.compositesb.2020.108211>.
- [13] A. Aabid et al., "A Systematic Review of Piezoelectric Materials and Energy Harvesters for Industrial Applications," *Sensors*, vol. 21, no. 12, p. 4145, Jun. 2021, doi: <https://doi.org/10.3390/s21124145>.
- [14] N. Sezer and M. Koç, "A comprehensive review on the state-of-the-art of piezoelectric energy harvesting," *Nano Energy*, vol. 80, p. 105567, Feb. 2021, doi: <https://doi.org/10.1016/j.nanoen.2020.105567>.
- [15] Çiftçi B. Ç., G. Kaya, and M. Kurt, "Analysis of Acoustic Signals of Footsteps from the Piezoelectric Sensor," *Journal of Advanced Research in Natural and Applied Sciences*, vol. 9, no. 4, pp. 931–

- 937, Dec. 2023, doi: <https://doi.org/10.28979/jarnas.1307466>.
- [16] M. Strantza, D. Van Hemelrijck, P. Guillaume, and D. G. Aggelis, "Acoustic emission monitoring of crack propagation in additively manufactured and conventional titanium components," *Mechanics Research Communications*, vol. 84, pp. 8–13, Sep. 2017, doi: <https://doi.org/10.1016/j.mechrescom.2017.05.009>.
- [17] W. Mu, Y. Gao, Y. Wang, G. Liu, and H. Hu, "Modeling and Analysis of Acoustic Emission Generated by Fatigue Cracking," *Sensors*, vol. 22, no. 3, pp. 1208–1208, Feb. 2022, doi: <https://doi.org/10.3390/s22031208>.
- [18] T. I. Khan, A. A. Rashid, and T. Nanami, "Theoretical and experimental analysis of acoustic emission signal for resonant sensor on homogenous material," *Sensing and Bio-Sensing Research*, vol. 39, p. 100550, Feb. 2023, doi: <https://doi.org/10.1016/j.sbsr.2023.100550>.
- [19] M. A. Aulestia, R. Gotz, Paulo, F. A. Alexandre, B. O. Fernandez, and Pedro Oliveira Junior, "A Low-Cost Acoustic Emission Sensor based on Piezoelectric Diaphragm," *IEEE Sensors Journal*, pp. 1–1, Jan. 2020, doi: <https://doi.org/10.1109/jsen.2020.2988478>.
- [20] N. Chamankar, R. Khajavi, A. A. Yousefi, A. Rashidi, and F. Golestanifard, "A flexible piezoelectric pressure sensor based on PVDF nanocomposite fibers doped with PZT particles for energy harvesting applications," *Ceramics International*, vol. 46, no. 12, pp. 19669–19681, Aug. 2020, doi: <https://doi.org/10.1016/j.ceramint.2020.03.210>.
- [21] Ata Meshkinzar and A. M. Al-Jumaily, "Cylindrical Piezoelectric PZT Transducers for Sensing and Actuation," *Sensors*, vol. 23, no. 6, pp. 3042–3042, Mar. 2023, doi: <https://doi.org/10.3390/s23063042>.
- [22] W. R. Ali and M. Prasad, "Piezoelectric MEMS based acoustic sensors: A review," *Sensors and Actuators A: Physical*, vol. 301, p. 111756, Jan. 2020, doi: <https://doi.org/10.1016/j.sna.2019.111756>.
- [23] M. Abud, Mohanad Azzawi, and Hawazen Alnaqeeb, "A New Technique for Measuring Laser Pulse Energy Using PZT/SiO₂," *Journal of applied sciences and nanotechnology*, vol. 3, no. 2, pp. 87–96, Jun. 2023, doi: <https://doi.org/10.53293/jasn.2023.6122.1197>.
- [24] Park and J. Won, "Piezoelectric bedload impact sensor (PBIS) for particle size distribution.," Sep. 2015, doi: <https://doi.org/10.18297/etd/1095>.
- [25] M. Hayashi, Takuya Kikkawa, D. Koyama, and M. Matsukawa, "Piezoelectric particle sizer for measuring bed load using a combination of resonance vibration modes," *Sensors and Actuators A: Physical*, vol. 267, pp. 150–155, Nov. 2017, doi: <https://doi.org/10.1016/j.sna.2017.09.057>.
- [26] J.-F. Capsal, C. David, E. Dantras, and C. Lacabanne, "Piezoelectric sensing coating for real time impact detection and location on aircraft structures," *Smart Materials and Structures*, vol. 21, no. 5, p. 055021, May 2012, doi: <https://doi.org/10.1088/0964-1726/21/5/055021>.
- [27] P. J. Coghill, "Particle Size of Pneumatically Conveyed Powders Measured Using Impact Duration," *Particle & Particle Systems Characterization*, vol. 24, no. 6, pp. 464–469, Dec. 2007, doi: <https://doi.org/10.1002/ppsc.200601080>.
- [28] A. Boschetto and F. Quadri, "Powder size measurement by acoustic emission," *Measurement*, vol. 44, no. 1, pp. 290–297, Jan. 2011, doi: <https://doi.org/10.1016/j.measurement.2010.10.005>.
- [29] M. Uher and P. Benes, "Measurement of particle size distribution by the use of acoustic emission method," May 2012, doi: <https://doi.org/10.1109/i2mtc.2012.6229375>.
- [30] L. Gao, Y. Yan, R. M. Carter, D. Sun, P. Lee, and C. Xu, "On-line particle sizing of pneumatically conveyed biomass particles using piezoelectric sensors," *Fuel*, vol. 113, pp. 810–816, Nov. 2013, doi: <https://doi.org/10.1016/j.fuel.2012.12.029>.
- [31] Y. Hu, X. Huang, X. Qian, L. Gao, and Y. Yan, "Online particle size measurement through acoustic emission detection and signal analysis," May 2014, doi: <https://doi.org/10.1109/i2mtc.2014.6860883>.
- [32] M. Kobayashi, T. Miyachi, M. Hattori, S. Sugita, S. Takechi, and N. Okada, "Dust detector using piezoelectric lead zirconate titanate with current-to-voltage converting amplifier for functional advancement," *Earth, Planets and Space*, vol. 65, no. 3, pp. 167–173, Mar. 2013, doi:

- <https://doi.org/10.5047/eps.2012.08.011>.
- [33] James Robert Coombes and Y. Yan, "Experimental investigations into the use of piezoelectric film transducers to determine particle size through impact analysis," Kent Academic Repository (University of Kent), May 2016, doi: <https://doi.org/10.1109/i2mtc.2016.7520464>.
- [34] G. Zhang, Y. Yan, Y. Hu, and G. Zheng, "On-line size measurement of pneumatically conveyed particles through acoustic emission sensing," *Powder Technology*, vol. 353, pp. 195–201, Jul. 2019, doi: <https://doi.org/10.1016/j.powtec.2019.05.023>.
- [35] G. Zheng, Y. Yan, Y. Hu, and W. Zhang, "Online Measurement of the Size Distribution of Pneumatically Conveyed Particles Through Acoustic Emission Detection and Triboelectric Sensing," *IEEE transactions on instrumentation and measurement*, vol. 70, pp. 1–17, Jan. 2021, doi: <https://doi.org/10.1109/tim.2021.3062407>.
- [36] G. Zhang, Y. Yan, Y. Hu, and G. Zheng, "Investigations into the sensing mechanism of acoustic emission sensors for particle size measurement in a particular case: normal incidence," *Measurement science & technology*, vol. 32, no. 7, pp. 075107–075107, May 2021, doi: <https://doi.org/10.1088/1361-6501/abe338>.
- [37] E. Nsugbe, A. Starr, I. Jennions, and C. R. Carcel, "Particle Size Distribution Estimation of A Mixture of Regular and Irregular Sized Particles Using Acoustic Emissions," *Procedia Manufacturing*, vol. 11, pp. 2252–2259, 2017, doi: <https://doi.org/10.1016/j.promfg.2017.07.373>.
- [38] N. Çankaya, "Deriving Power Consumption Models from Energy Bills for Optimal Sizing of Hybrid Power in Commercial Buildings," *IEEE Access*, 2024, doi: <https://doi.org/10.1109/ACCESS.2024.3444710>